Published in final edited form as:
J Neurophysiol. 2008 June ; 99(6): 3136–3143. doi:10.1152/jn.91327.2007.

Artificial dirt: Microfluidic substrates for nematode neurobiology and behavior

S. R. Lockery[1], **K. J. Lawton**[1], **J. C. Doll**[2], **S. Faumont**[1], **S. M. Coulthard**[2], **T. R. Thiele**[1], **N. Chronis**[3], **K. E. McCormick**[1], **M. B. Goodman**[4], and **B. L. Pruitt**[2]

1 *Department of Biology, University of Oregon, Eugene, Oregon*

2 *Department of Mechanical Engineering, Stanford University, Stanford, California*

3 *Department of Mechanical Engineering, University of Michigan, Ann Arbor, Michigan*

4 *Department of Molecular and Cellular Physiology, Stanford University, Stanford, California*

Abstract

With a nervous system of only 302 neurons, the free-living nematode *Caenorhabditis elegans* is a powerful experimental organism for neurobiology. However, the laboratory substrate commonly used in *C. elegans* research, a planar agarose surface, fails to reflect the complexity of this organism's natural environment, complicates stimulus delivery, and is incompatible with high resolution optophysiology experiments. Here we present a new class of microfluidic devices for *C. elegans* neurobiology and behavior: agarose-free, micron-scale chambers and channels that allow the animals to crawl as they would on agarose. One such device mimics a moist soil matrix and facilitates rapid delivery of fluid-borne stimuli. A second device consists of sinusoidal channels that can be used to regulate the waveform and trajectory of crawling worms. Both devices are thin and transparent, rendering them compatible with high resolution microscope objectives for neuronal imaging and optical recording. Together, the new devices are likely to accelerate studies of the neuronal basis of behavior in *C. elegans*.

Keywords

C. elegans; soft lithography; chemosensation; locomotion; neuronal imaging

INTRODUCTION

With a nervous system of only 302 neurons, and a small repertoire of minimalist behaviors, the nematode worm *Caenorhabditis elegans* is a powerful system for neurobiology. However, the laboratory substrate most commonly used in *C. elegans* research—an agarose-filled Petri plate—has four potentially serious limitations. First, an exposed agarose surface is very different from the habitats in which *C. elegans* is found in the wild which include soil, compost, leaf and fruit litter, and several invertebrate hosts (Sudhaus and Kiontke 1996; Barriere and Felix 2005; Kiontke and Sudhaus 2006; Barriere and Felix 2007). Second, it is difficult to regulate ecologically important stimulus parameters such as solute and odorant concentration (Ward 1973; Bargmann and Horvitz 1991), temperature (Hedgecock and Russell 1975), osmolarity (Culotti and Russell 1978), and oxygen partial pressure (Gray et al. 2004) in the bulk agarose or on its surface. Third, neither the trajectory nor the waveform of individual

Correspondence: Dr. Shawn Lockery, 305 Huestis Hall, 1210 University of Oregon, Eugene, OR 97403-1210, Phone: (541) 346-4590, Email: E-mail: shawn@uoregon.edu.

worms is under experimental control. Fourth, agarose-filled plates are incompatible with the high magnification, high numerical aperture microscope objectives required to resolve the minute, closely spaced neurons of this species and to optimize signal-to-noise ratios in optophysiological experiments (Kerr et al. 2000; Nagel et al. 2005). Thus, *C. elegans* behavioral neurobiology would be accelerated by the introduction of a more naturalistic substrate that is amenable to experimental manipulations and imaging single cells.

A promising new approach to constructing substrates for nematode research is soft lithography, a microfluidic fabrication technique in which a transparent elastomer is cast against a mold that contains a negative version of the desired features (Sia and Whitesides 2003; Whitesides 2006). Soft lithography fits hand-and-glove with *C. elegans* research in three significant respects. First, because the technique is based on high-resolution photolithography, one can easily build devices with arbitrarily shaped features (channels, chambers, ports, etc.) that match the size and shape of a microscopic worm. Second, the elastomer, polydimethylsiloxane (PDMS), is both optically transparent and gas-permeable, so the worm remains visible and viable. Third, fluid flow within microfluidic channels is laminar, a property that can be exploited to create local gradients and deliver fluid borne stimuli with unusual precision.

Recently, several research groups have capitalized on the advantages of soft lithography to create devices that facilitate nematode research at a range of feature scales. At the microscopic scale, it has been used to build devices for worm restraint (Chronis et al. 2007), optofluidic imaging (Heng et al. 2006), automated sorting and screening (Rohde et al. 2007), neuronal ablations (Hulme et al. 2007), and localized chemical stimulation (Chalasani et al. 2007). In devices at this scale, the worms are confined to close-fitting channels which, by design, prevent locomotion. At the macroscopic scale, soft lithography has been used to create long-term culture systems (Nahui et al. 2007), structured agarose baths for swimming worms (Hwang et al. 2007), and several types of two-dimensional mazes for behavioral choice experiments (Zhang et al. 2005; Qin and Wheeler 2007). Here we present a new class of microfluidic devices for *C. elegans* research: agarose-free, micron-scale chambers and channels that allow the animals to crawl as they would on agarose, yet are compatible with optical recording at high numerical aperture.

We present two such devices. The first, which we refer to as the artificial soil device, consists of a fluid-filled matrix of microscopic posts that mimic soil particles. The second, which we refer to as the waveform sampler device, contains a set of sinuous microfluidic channels with a variety of amplitudes and wavelengths. Here we show that worms crawl with ease through both devices and we present novel experimental manipulations that can be performed to investigate sensory and motor behaviors in *C. elegans*.

METHODS

Animals

Nematodes (*C. elegans*, Bristol N2) were grown in mixed-staged cultures at 22.5 C on 1.7% agarose-filled plates containing nematode growth medium seeded with *Escherichia coli* strain OP50 (Brenner 1974). All experiments were performed at room temperature (20–23 C) on adult worms. Neurons were labeled with for fluorescence imaging (Fig. 7) using an *odr-2b*::YC3.60 construct which was prepared by standard procedures (Mello et al. 1991).

Solutions

Chambers and channels were filled with buffered saline containing (in mM): 20 NaCl, 0.5 $CaCl_2$, 0.5$MgS0_4$, 5 HEPES (pH 7.1) and glycerol to a final osmolarity of 175 mOsm. In the step-response assay (Fig. 4), the high NaCl solution contained (in mM): 100 NaCl, 1 $CaCl_2$, 1

$MgS0_4$, 10 HEPES (pH 7.1). The low NaCl solution was the same except that it contained only 1 mM NaCl. Both solutions were balanced to a final osmolarity of 187 mOsm using glycerol.

Device fabrication

We fabricated the devices using standard soft lithography (Sia and Whitesides 2003). Briefly, we used a transparency mask (ArtNetPro, San Jose, CA) to pattern features in a 50 μm thick layer of SU-8 photoresist (SU-8 2035, MicroChem, Newton, MA) on a silicon wafer (University Wafer, South Boston, MA) to form a master. Feature height was determined by the thickness of the SU-8 layer. The master was used as a template for molding devices in polydimethylsiloxane (PDMS, Sylgard 184, Dow Corning, Corning, NY). Chlorotrimethylsilane (Sigma-Aldrich, St. Louis, MO), vapor deposited for 2 min at atmospheric pressure, was used as a releasing agent. PDMS prepolymer was cast against the master and cured in an oven for 1 hr at 100 C. After removing the PDMS from the template, fluid inlet and outlet holes, as well as worm injection ports, were punched with a sharpened stub needle (0.070 mm O.D., 22 G). Devices were irreversibly bonded to 1 mm thick glass plates (Bio-Rad, Hercules, CA) after pre-exposure to oxygen plasma (120 W, 2 sec). Each inlet and outlet was fitted with a short stainless steel tube (12.7 mm length, 0.62 mm 0.D., 0.43 mm I.D.; New England Small Tube, Litchfield, NH) to which polyethylene tubing (0.99 mm O.D, 0.58 mm I.D., Scientific Commodities, Lake Havasu City, AZ) was attached to establish fluid connections. To load a worm into the device, we first sucked the animal into the tip of a length of polyethylene tubing using a 1 cc syringe. We then connected the tubing to the device and applied gentle pressure. Worms were removed from the waveform device by fluid pressure from the same syringe. However, this method did not work with the artificial soil device because pressure on the worm was insufficient to overcome the resistance provided by the pillars. Accordingly, to remove worms from the artificial soil device we first broke them up by sonication (10–20 min), then flushed the device with water.

Step-response assay

Single worms were transferred to the artificial soil device (post diameter 100 μm; minimum gap 100 μm) and allowed to accommodate to perfusion (0.65 mL/min) in the device for 2 min before the experiment began. The behavior of individual worms was scored by an observer who pressed computer keys to record the time of entry into two locomotory states: forward and reverse; the omega-turn state was included in the forward state. The behavior of individual worms was quantified as the probability of forward locomotion obtained by computing the fraction of time the worm resided in the forward state in consecutive 10 sec bins. The behavior of control and experimental groups was summarized by computing bin-wise means of individual forward probabilities.

RESULTS

The artificial soil device

The artificial soil device consists of a 1 x 1 cm hexagonal array of cylindrical posts, 50 μm in height, formed by casting PDMS against a photolithographic mold (Fig. 1). The PDMS is irreversibly bonded to a glass plate, which serves as a floor, forming an enclosed chamber. The worm inhabits fluid filled spaces between posts, which mimic soil particles or other contact points that provide reaction forces for crawling in natural environments. The device is perfused via fluid reservoirs connected to the inlet and flow rate is regulated by a peristaltic pump that draws from the outlet. The perfusion solution is switched by means of manual valves. Worms are inserted using a fluid-filled syringe fitted with a small tube connected to one of four funnel-shaped injection ports (Chronis et al. 2007). Because the height of the chamber is less than 80 μm, the diameter of an adult worm (White et al. 1986), the worm is slightly compressed; this

feature facilitates neuronal imaging by reducing *z*-axis displacement of cells as the animal moves.

C. elegans propels itself mainly by undulatory crawling, in which thrust is produced by a wave of muscular contraction and relaxation as it travels along the body. On an undifferentiated agarose surface, *C. elegans* locomotion exhibits four main characteristics (Croll 1975a; b): (1) Worms lie on their right or left side such that undulations are dorsoventral. (2) Instantaneous body posture is sinuous and frequently sinusoidal. (3) Locomotion is smooth and continuous, like gliding. (4) Locomotion involves three main states: forward crawling, in which the wave travels from head to tail; reverse crawling, in which the wave travels from tail to head; and the so-called omega turn, defined as head-to-body contact while animal is moving forward.

We found that worms crawled without difficulty in the artificial soil device (Fig. 2B,C). Crawling persisted for three hours, the longest observation time in this study, which provides a lower bound on longevity in the device. Movement was undulatory and involved dorsoventral bends, as detected by noting the orientation of body bends with respect to ventral features such as the vulva. Instantaneous body posture was sinuous, but less frequently sinusoidal than on agarose, especially when the worm selected an alley between rows of posts (Fig. 2B, elapsed time 7–17 sec). Movement was smooth and continuous (Supplemental Movies 1, 2), and all three locomotory states were evident (Fig. 2B,C and Supplemental Movies 1, 2). We conclude that crawling in the artificial soil chip exhibits the main characteristics of crawling on an agarose surface (Croll 1975a; b).

The topography of an hexagonal array of posts is defined by their diameter and the minimum gap between them. To explore the range of topographies through which worms can crawl, we fabricated nine devices, each with a unique combination of diameter and gap (Fig. 3). We found that worms crawled with ease through each device, indicating that crawling does not depend on a narrow range of topographies. Topography also affected the pressure required for fluid flow within the device by altering the cross sectional open area. The array shown in Fig. 3C had the greatest open area and thus required the lowest pressure for fluid flow. Crawling speed in this array was 0.14 ± 0.017 mm/sec (SEM, 3 forward bouts in each of 5 animals), which is close to the speed of worms crawling on foodless agarose surfaces: 0.2–0.250 mm/sec (Pierce-Shimomura et al. 1999;Ryu and Samuel 2002). Thus the array most suited to fluid flow promotes crawling at essentially normal speeds.

Previous work has shown that stepwise changes in the concentration of NaCl, a potent chemoattractant in *C. elegans* (Ward 1973), elicit transient changes in the frequency of turning behaviors (Dusenbery 1980), a response that contributes to chemotaxis in steep gradients (Miller et al. 2005). We used NaCl step-response behavior to test whether normal sensory responses could be produced using the artificial soil device. To facilitate fluid flow in these experiments, we used the artificial soil device with the largest open area (Fig. 3C). A single trial involved adapting the worm for three minutes to perfusion at 100 mM NaCl (Fig. 1, reservoir A), then switching to perfusion at 1 mM NaCl (reservoir B) and monitoring the probability of forward locomotion. In parallel experiments to control for mechanical artifacts caused by subtle pressure changes that might occur during switching, both perfusion channels contained 100 mM NaCl (reservoirs A and C). To establish a fixed interval between switching the valves and the solution change experienced by the worm, a length of tubing was inserted between the junction and the inlet, as indicated in Fig. 1A, resulting in a 5 sec delay between valve adjustment and the arrival of the solution front at the center of the chamber.

As expected, a downward step in NaCl concentration transiently reduced the probability of forward locomotion (Fig. 4). No response was seen in the control experiment indicating that pressure changes, if they occurred, were not behaviorally relevant. The amplitude and time

course of the depression in forward probability was consistent with previous observations of the response to similar concentration changes when worms are crawling on agarose-coated membranes (Miller et al. 2005). We conclude that the *C. elegans* chemosensory responses are intact in the artificial soil device. Thus the device provides a new means of precisely regulating the sensory environment of unrestrained, freely crawling worms.

The waveform sampler device

The basic element of the waveform sampler is a sinusoidal channel, 50 μm in height, with worm injection ports at the ends (Fig. 5). The waveform device, like the artificial soil device, is a PDMS casting bonded to a glass plate to form an array of variously shaped channels. Each channel design has three sinusoidal domains with a common amplitude but different wavelengths. Channel designs were replicated in triplicate with widths of 60, 80, and 100 μm because the best width could not be predicted in advance. After filling the desired channel with fluid, the worm is inserted using a fluid-filled syringe fitted with a small tube that can be connected to one of the ports. After insertion, the worm is deposited into the domain of choice by pushing or pulling on the syringe; the straight segments between domains prevent the worm from crawling between them.

We tested a set of six channels (Fig. 5). In this set, channel amplitudes ranged from 0.5 to 2 times the peak-to-peak amplitude A (200 μm) of a wild type worm crawling on an agarose surface in the presence of bacterial food (Cronin et al. 2005), whereas wavelengths ranged from 0.4 to 3 times the nominal wild type wavelength λ (500 μm). The latter value was in the middle of the wavelength range (400–600 μm) for worms crawling in the presence of food (Kawasaki et al. 1999;Cronin et al. 2005). For the adult worms used in this study, the best results were usually obtained with the 80 μm channels; the 60 μm channels were often too tight to permit movement, whereas the 100 μm channels were generally too loose to restrict movements to the waveform prescribed by the shape of the channel. The cross-sectional area of the 80 μm channels (4000 μm^2) was less than the cross-sectional area of the mid-body of an adult worm (5027 μm^2); thus the worm was compressed against the top, bottom, and sides of the channel. This aspect of design helps to ensures good control of crawling waveform in addition to reducing z-axis movements of cells, as in the case of the artificial soil device.

In a survey of crawling in each of the channels, we found three distinct types of domains (Fig. 5). (1) In the domains shown in green, worms were able to crawl and the worm's waveform matched the amplitude and wavelength of the channel. (2) In the domains shown in blue, worms were also able to crawl, but the worm's waveform amplitude was significantly less than the amplitude of the channel. This situation occurred because the effective width of the channel is increased in the tight turns at the channel peaks where adjacent channel segments on the inside of the turns overlap (Supplemental Fig. 1A). (3) In the domains shown in red, worms were unable to move. Following Gray's theoretical analysis of undulatory locomotion (Gray 1953), the maximum tangential thrust F exerted by a half-wave obeys the proportionality

$$F \propto \frac{2\pi A/\lambda}{\lambda\sqrt{1+2\pi(A/\lambda)^2}}.$$

The three domains in which worms were unable to move correspond to the domains with the lowest F values in the device. It seems likely, therefore, that in these domains worms were unable to generate sufficient thrust to overcome the friction that results from contact with the channel walls.

Using the green domains, we were able to experimentally control both wavelength and amplitude of robustly crawling individuals. For 80 μm channels, the effective range was from 1.0*A*, 2.0λ at the low-*F* limit, to 0.5*A*, 0.6 λ at the high-*F* limit. Examples of crawling with controlled waveforms are shown in Fig. 6 (see also Supplemental Movies 3, 4, and 5). In the waveform of a wild-type worm crawling on a conventional agarose substrate there are typically three peaks per body length (Fig. 2A). However, by experimentally manipulating waveform, we found that worms can crawl with ease when there is only one (Fig. 6B) or when there are as many as five peaks per body length (Fig. 6C). This result implies that the mechanism for generation and propagation of the undulatory wave for crawling is independent of wavelength over a wide range, which may reflect an adaptation for crawling through complex, irregular natural substrates.

Imaging

C. elegans presents two main challenges in optical recording experiments using fluorescent probes (Kerr et al. 2000). First, because they are quite small (2 μm diam.), the cell bodies of *C. elegans* neurons contain a small amount of the probe and thus emit relatively few photons; this problem reduces the optical signal-to-noise ratio. Second, because the neurons are often closely packed (White et al. 1986), it can be difficult to resolve individual neurons. Both problems would be addressed most effectively by the use of high magnification, high numerical aperture microscope objectives. To demonstrate that the artificial soil and waveform sampler devices are compatible with such objectives, we bonded each device to a coverslip instead of a glass plate. We then imaged fluorescently labeled neurons as one might in an optophysiology experiment: with a conventional (non-confocal) microscope fitted with a 63x/1.4 NA oil immersion objective (Fig. 7). Using a strain in which the calcium sensor cameleon (Miyawaki et al. 1997) is expressed under the control of the *odr-2b* promoter (Gray et al. 2005) which labels a small number of sensory neurons and interneurons in the head, we were able to clearly resolve individual, closely spaced neuron somata in both devices. Thus the new devices should facilitate optical recording experiments that require stimulus delivery or waveform and trajectory control in freely crawling nematodes.

DISCUSSION

Here we present two types of agarose-free, micron-scale devices that allow nematodes to crawl as they would on agarose. Although the first device is specialized for stimulus delivery and the second device is specialized for waveform and trajectory control, both devices have a range of other uses.

The artificial soil device

The artificial soil device is likely to accelerate investigations of the behavior of *C. elegans* and its neuronal basis in three main respects.

1. The device provides a means of observing behavior in substrates that are more complex and, in some respects, more realistic than an agarose surface. The range of natural substrates that *C. elegans* frequents is not yet fully described (Kiontke and Sudhaus 2006). However, sinusoidal locomotion on a smooth, undifferentiated agarose substrate almost certainly represents an idealized case. By contrast, in natural substrates in which *C. elegans* has been found so far, locomotion is likely to deviate significantly from this ideal because the worm must thread its way through a labyrinth of randomly distributed, closely packed obstacles. Thus it is reasonable to suppose that locomotion in natural substrates is far more complex than on agarose and, because natural substrates are opaque, much of this complexity may have been missed. The artificial soil device provides a means for recreating at least some of this complexity

in a transparent planar structure in which behavior can be directly observed and quantified. Such an approach replicates the complexity of natural substrates more conveniently and reproducibly than previous approaches for creating structured crawling environments, such as coating agarose with sand (Anderson et al. 1997).

2. The device expands the range of substrate topographies that can be investigated. Here we studied worms crawling in a regular array of uniformly shaped posts, but artificial soil devices are, because of their photolithographic origin, almost infinitely configurable. For example, one could systematically manipulate the size, shape, and spatial distribution of the posts to produce customized substrates for testing theories of how thrust generation is related to body posture, or for investigating new aspects of behaviors such as the transition between crawling and swimming, or thigmotaxis and rheotaxis, forms of spatial orientation that depend on the extent of animal-substrate contact or current flow, respectively (Fraenkel and Gunn 1940). Alternatively, one could fabricate devices from micrographs of cross-sections of various natural substrates.

3. The device provides a new means of precisely regulating the amplitude, spatial distribution, and timing of ethologically relevant stimulus parameters such as tastants, odorants, temperature, viscosity, and oxygen partial pressure. The key advance provided by the device is the ability to induce crawling in submerged worms, which otherwise would swim. This advance is significant because it makes presenting a change in sensory input during free crawling a simple matter of selective perfusion. The new method is more convenient that previous methods such as the so-called concentration clamp (Miller et al. 2005) in which the step is produced by exchanging fluids beneath an agarose-coated, microporous membrane. Also, with the addition of multiple perfusion lines, temporally complex stimuli such as ramps or pseudorandom inputs could be delivered; the latter would make it possible to use reverse correlation techniques (Rieke et al. 1997) to study sensory encoding. Here we used the artificial soil device to deliver changes in sensory input, but the device could also be used for controlled delivery of pharmacological agents, nutrients, and other experimental reagents.

The artificial soil device currently has three main limitations. First, the elastomer out of which the device is constructed mimics the microscopic structure of natural substrates but not their chemical properties. Second, the device is planar rather than three-dimensional, so it is not possible to investigate movements along all three axes simultaneously. Third, worms cannot be recovered intact from the device (see Methods). The first limitation can be partly addressed by taking advantage of the fact that functional groups are easily attached to PDMS surfaces (Hu et al.; Huang et al. 2006). The second limitation can be addressed using multilayer fabrication techniques (Abgrall et al. 2006; Tsang et al. 2007). The third limitation could be addressed by reversibly bonding the PDMS to the glass using a clamp.

The waveform sampler device

The waveform sampler device is likely to have applications at two distinct spatial scales.

1. At the micrometer scale (10–100 μm), the device allows one to experimentally manipulate the waveform of crawling worms. This feature should make it possible to test theoretical predictions concerning the relationship between waveform and undulatory thrust (Gray 1953). The device can also be used to induce a specific spatiotemporal pattern of body postures by forcing a worm through a channel using hydrostatic pressure (Lockery, unpublished). Such manipulations could be useful for investigations of the neuronal basis of proprioception (Liu et al. 1996; Li et al. 2006).

2. At the centimeter scale (1–10 cm), the device provides a means to control the trajectory of a crawling worm. Trajectory control could be used to simplify automated behavioral tracking experiments (Williams and Dusenbery 1990; Waggoner et al. 1998; Pierce-Shimomura et al. 1999), by reducing a two-dimensional tracking problem to, in effect, a one-dimensional problem. Such tasks include optical recording and targeting worms for photostimulation (Nagel et al. 2005). Another application is what might be termed a behavioral replay experiment. Here an image of the trajectory of a freely crawling worm can be captured and reproduced as a microfluidic sinusoidal channel (Lockery, unpublished). Using this approach one could, for example, induce wild-type worms to follow the tracks of mutant worms and *vice versa*.

Imaging

A behavior that closely resembles crawling can be induced in a submerged worm by compressing the animal in a low profile chamber, called the behavior chip, that is slightly wider than the worm (Chronis et al. 2007). Like the devices described here, the behavior chip is bonded to a coverslip, making it compatible with high numerical aperture, high magnification microscope objectives. In contrast to its behavior in the artificial soil and waveform sampler devices, the worm does not actually translocate in the behavior chip because it has nothing to push against. As a consequence, the worm likely experiences proprioceptive and exteroceptive inputs that are somewhat different from those of a moving worm, which could be a disadvantage in some experiments. However, the behavior chip has the advantage that because the worm is effectively stationary, a tracking system is not needed to keep it in view in optophysiology experiments (Clark et al. 2007).

Conclusion

The artificial soil and waveform sampler devices add important new features to the microfluidic toolkit for experimental investigations of *C. elegans.* These features include a closer match to the microscopic structure of natural substrates, temporally and spatially precise delivery of a wide range of stimuli to freely crawling worms, and experimental control of locomotion waveform and trajectory. Significantly, both devices can be made compatible with high magnification, high numerical aperture microscope objectives. Thus, combined with a tracking system, the new devices could make it possible to resolve minute, closely spaced neurons in optophysiological experiments in freely crawling nematodes. Finally, the new devices can readily be incorporated into multi-component microfluidic systems for high throughput screening of locomotion phenotypes in response to neuronal ablations, mutations, and novel pharmacological agents (Hulme et al. 2007; Nahui et al. 2007; Rohde et al. 2007).

Supplementary Material

Refer to Web version on PubMed Central for supplementary material.

Acknowledgments

GRANTS

This work was supported by National Institute of Mental Health Grant NIMH-051383, and the National Science Foundation Grant IOS-0543643

References

Abgrall P, Christine Lattes C, Conedera V, Dollat X, Colin S, Gu AM. A novel fabrication method of flexible and monolithic 3D microfluidic structures using lamination of SU-8 films. Journal of Micromechanics and Microengineering 2006;16:113–121.

Anderson ARA, Young IM, Sleeman BD, Griffiths BS, Robertson WM. Nematode movement along a chemical gradient in a structurally heterogenous environment. 1. Experiment. Fundamental and applied nematology 1997;20:157–163.

Bargmann CI, Horvitz HR. Chemosensory neurons with overlapping functions direct chemotaxis to multiple chemicals in C. elegans. Neuron 1991;7:729–742. [PubMed: 1660283]

Barriere A, Felix MA. High local genetic diversity and low outcrossing rate in Caenorhabditis elegans natural populations. Curr Biol 2005;15:1176–1184. [PubMed: 16005289]

Barriere A, Felix MA. Temporal dynamics and linkage disequilibrium in natural Caenorhabditis elegans populations. Genetics 2007;176:999–1011. [PubMed: 17409084]

Brenner S. The genetics of Caenorhabditis elegans. Genetics 1974;77:71–94. [PubMed: 4366476]

Chalasani SH, Chronis N, Tsunozaki M, Gray JM, Ramot D, Goodman MB, Bargmann CI. Dissecting a circuit for olfactory behaviour in Caenorhabditis elegans. Nature 2007;450:63–70. [PubMed: 17972877]

Chronis N, Zimmer M, Bargmann CI. Microfluidics for in vivo imaging of neuronal and behavioral activity in Caenorhabditis elegans. Nature methods 2007;4:727–731. [PubMed: 17704783]

Clark DA, Gabel CV, Gabel H, Samuel AD. Temporal activity patterns in thermosensory neurons of freely moving Caenorhabditis elegans encode spatial thermal gradients. J Neurosci 2007;27:6083–6090. [PubMed: 17553981]

Croll NA. Behavioural analysis of nematode movement. Adv Parasit 1975a;13:71–122.

Croll NA. Components and patterns in the behavior of the nematode Caenorhabditis elegans. J Zool 1975b;176:159–176.

Cronin CJ, Mendel JE, Mukhtar S, Kim YM, Stirbl RC, Bruck J, Sternberg PW. An automated system for measuring parameters of nematode sinusoidal movement. BMC Genet 2005;6:5. [PubMed: 15698479]

Culotti J, Russell R. Osmotic avoidance defective mutants of the nematode C. elegans. Genetics 1978;90:243–256. [PubMed: 730048]

Dusenbery DB. Responses of the nematode Caenorhabditis elegans to controlled chemical stimulation. Journal of Comparative Physiology 1980;136:127–331.

Fraenkel, GS.; Gunn, DL. The Orientation of Animals. Oxford: Oxford University Press; 1940.

Gray J. Undulatory propulsion. Quarterly Journal of Microscopical Science 1953;94:551–578.

Gray JM, Hill JJ, Bargmann CI. A circuit for navigation in Caenorhabditis elegans. Proc Natl Acad Sci U S A 2005;102:3184–3191. [PubMed: 15689400]

Gray JM, Karow DS, Lu H, Chang AJ, Chang JS, Ellis RE, Marletta MA, Bargmann CI. Oxygen sensation and social feeding mediated by a C. elegans guanylate cyclase homologue. Nature 2004;430:317–322. [PubMed: 15220933]

Hedgecock EM, Russell RL. Normal and mutant thermotaxis in the nematode Caenorhabditis elegans. Proceedings of the National Academy of Science 1975;72:4061–4065.

Heng X, Erickson D, Baugh LR, Yaqoob Z, Sternberg PW, Psaltis D, Yang C. Optofluidic microscopy--a method for implementing a high resolution optical microscope on a chip. Lab Chip 2006;6:1274–1276. [PubMed: 17102839]

Hu S, Ren X, Bachman M, Sims CE, Li GP, Allbritton N. Surface modification of poly(dimethylsiloxane) microfluidic devices by ultraviolet polymer grafting. Analytical Chemistry 2002;74:4117–4123. [PubMed: 12199582]

Huang B, Wu H, Kim S, Kobilkac BK, Zare RN. Phospholipid biotinylation of polydimethylsiloxane (PDMS) for protein immobilization. Lab on a Chip 2006;6:369–373. [PubMed: 16511619]

Hulme SE, Shevkoplyas SS, Apfeld J, Fontana W, Whitesides GM. A microfabricated array of clamps for immobilizing and imaging C. elegans. Lab Chip 2007;7:1515–1523. [PubMed: 17960280]

Hwang, H.; Nam, S.; Martinez; Austin, RH.; Ryu, WS.; Park, S. Enhanced locomotion Caenorhabditis elegans [sic] in structured microfluidic environments. International Conference on Miniaturized Systems for Chemistry and Life Sciences; Paris, France. 2007. p. 131-133.

Kawasaki M, Hisamoto N, Iino Y, Yamamoto M, Ninomiya-Tsuji J, Matsumoto K. A Caenorhabditis elegans JNK signal transduction pathway regulates coordinated movement via type-D GABAergic motor neurons. Embo J 1999;18:3604–3615. [PubMed: 10393177]

Kerr R, Lev-Ram V, Baird G, Vincent P, Tsien RY, Schafer WR. Optical imaging of calcium transients in neurons and pharyngeal muscle of C. elegans. Neuron 2000;26:583–594. [PubMed: 10896155]

Kiontke, K.; Sudhaus, W., editors. Ecology of Caenorhabditis species. 2006.

Li W, Feng Z, Sternberg PW, Xu XZ. A C. elegans stretch receptor neuron revealed by a mechanosensitive TRP channel homologue. Nature 2006;440:684–687. [PubMed: 16572173]

Liu J, Schrank B, Waterston RH. Interaction between a putative mechanosensory membrane channel and a collagen. Science 1996;273:361–364. [PubMed: 8662524]

Mello CC, Kramer JM, Stinchcomb D, Ambros V. Efficient gene transfer in C. elegans: extrachromosomal maintenance and integration of transforming sequences. Embo J 1991;10:3959–3970. [PubMed: 1935914]

Miller AC, Thiele TR, Faumont S, Moravec ML, Lockery SR. Step-response analysis of chemotaxis in Caenorhabditis elegans. J Neurosci 2005;25:3369–3378. [PubMed: 15800192]

Miyawaki A, Llopis J, Heim R, McCaffery JM, Adams JA, Ikura M, Tsien RY. Fluorescent indicators for Ca2+ based on green fluorescent proteins and calmodulin. Nature 1997;388:882–887. [PubMed: 9278050]

Nagel G, Brauner M, Liewald JF, Adeishvili N, Bamberg E, Gottschalk A. Light activation of channelrhodopsin-2 in excitable cells of Caenorhabditis elegans triggers rapid behavioral responses. Curr Biol 2005;15:2279–2284. [PubMed: 16360690]

Nahui K, Dempsey CM, Zoval JV, Sze J-Y, Madou MJ. Automated microfluidic compact disc (CD) cultivation system of Caenorhabditis elegans. Science Direct, Sensors and Actuators B 2007;122:511–518.

Pierce-Shimomura JT, Morse TM, Lockery SR. The fundamental role of pirouettes in Caenorhabditis elegans chemotaxis. J Neurosci 1999;19:9557–9569. [PubMed: 10531458]

Qin J, Wheeler AR. Maze exploration and learning in C. elegans. Lab Chip 2007;7:186–192. [PubMed: 17268620]

Rieke, FM.; Warland, D.; de Ruyter van Steveninck, R.; Bialek, W. Spikes: Exploring the Neural Code. Cambridge, MA: MIT Press; 1997.

Rohde CB, Zeng F, Gonzalez-Rubio R, Angel M, Yanik MF. Microfluidic system for on-chip high-throughput whole-animal sorting and screening at subcellular resolution. Proc Natl Acad Sci U S A 2007;104:13891–13895. [PubMed: 17715055]

Ryu WS, Samuel AD. Thermotaxis in Caenorhabditis elegans analyzed by measuring responses to defined Thermal stimuli. J Neurosci 2002;22:5727–5733. [PubMed: 12097525]

Sia SK, Whitesides GM. Microfluidic devices fabricated in poly(dimethylsiloxane) for biological studies. Electrophoresis 2003;24:3563–3576. [PubMed: 14613181]

Sudhaus W, Kiontke K. Phylogeny of Rhabditis subgenus Caenorhabditis (Rhabditidae, Nematoda). Journal of Zoological Systematics and Evolutionary Research 1996;34:217–233.

Tsang VL, Chen AA, Cho LM, Jadin KD, Sah RL, DeLong S, West JL, Bhatia SN. Fabrication of 3D hepatic tissues by additive photopatterning of cellular hydrogels. FASEB Journal 2007;21:790–801. [PubMed: 17197384]

Waggoner LE, Zhou GT, Schafer RW, Schafer WR. Control of alternative behavioral states by serotonin in Caenorhabditis elegans. Neuron 1998;21:203–214. [PubMed: 9697864]

Ward S. Chemotaxis by the nematode Caenorhabditis elegans: identification of attractants and analysis of the response by use of mutants. Proc Natl Acad Sci U S A 1973;70:817–821. [PubMed: 4351805]

White JG, Southgate E, Thomson JN, Brenner S. The structure of the nervous system of the nematode Caenorhabditis elegans. Philos Trans R Soc Lond B Biol Sci 1986;314:1–340.

Whitesides GM. The origins and future of microfluidics. Nature 2006;442:368–373. [PubMed: 16871203]

Williams PL, Dusenbery DB. A promising indicator of neurobehavioral toxicity using the nematode Caenorhabditis elegans and computer tracking. Toxicology and industrial health 1990;6:425–440. [PubMed: 2237928]

Zhang Y, Lu H, Bargmann CI. Pathogenic bacteria induce aversive olfactory learning in Caenorhabditis elegans. Nature 2005;438:179–184. [PubMed: 16281027]

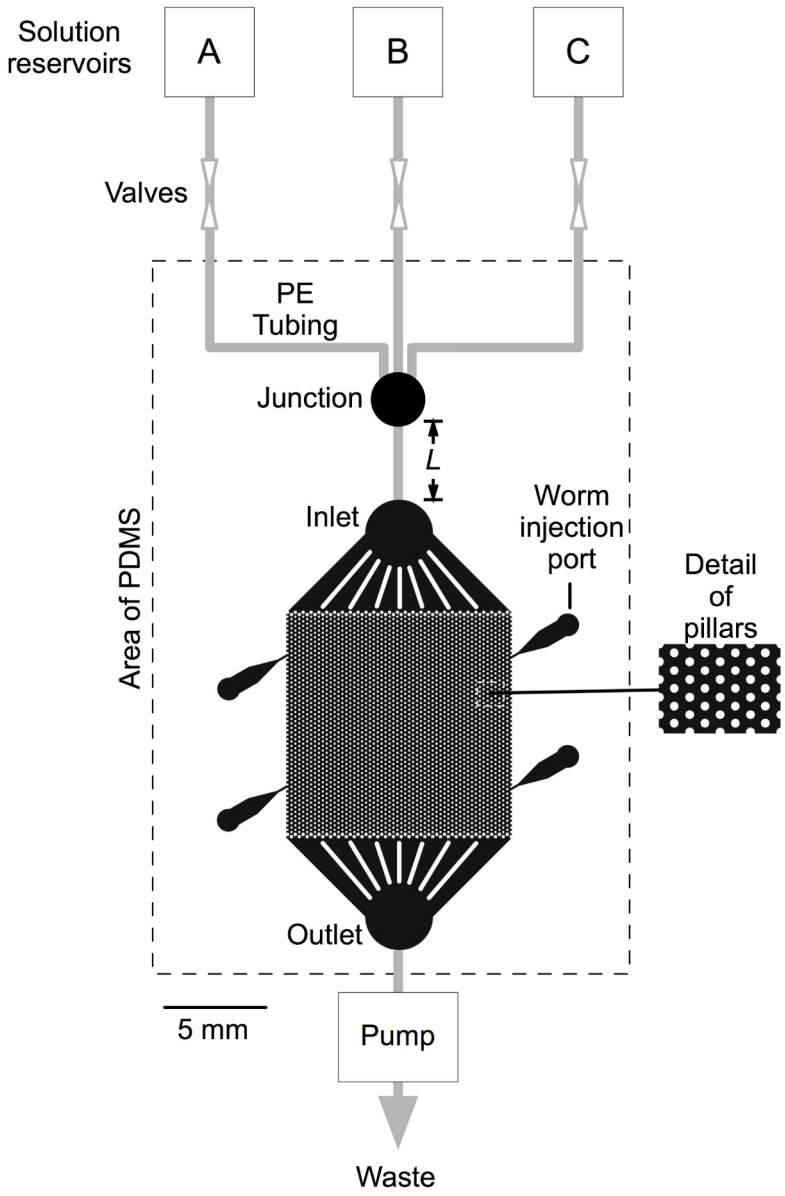

Figure 1.
Diagram of the artificial soil device. The broken line indicates the molded PDMS component. Within this region, the color black indicates spaces that are open to fluid flow. The worm is injected via one of four injection ports and crawls among microscopic posts in the central region, which measures 1 x 1 cm. The device is fed by three fluid reservoirs (A–C). Gray lines indicate polyethylene tubing. A piece of tubing of variable length *L*, inserted between the junction and the inlet, provides for an adjustable delay between switching the valves and the solution change experienced by the worm.

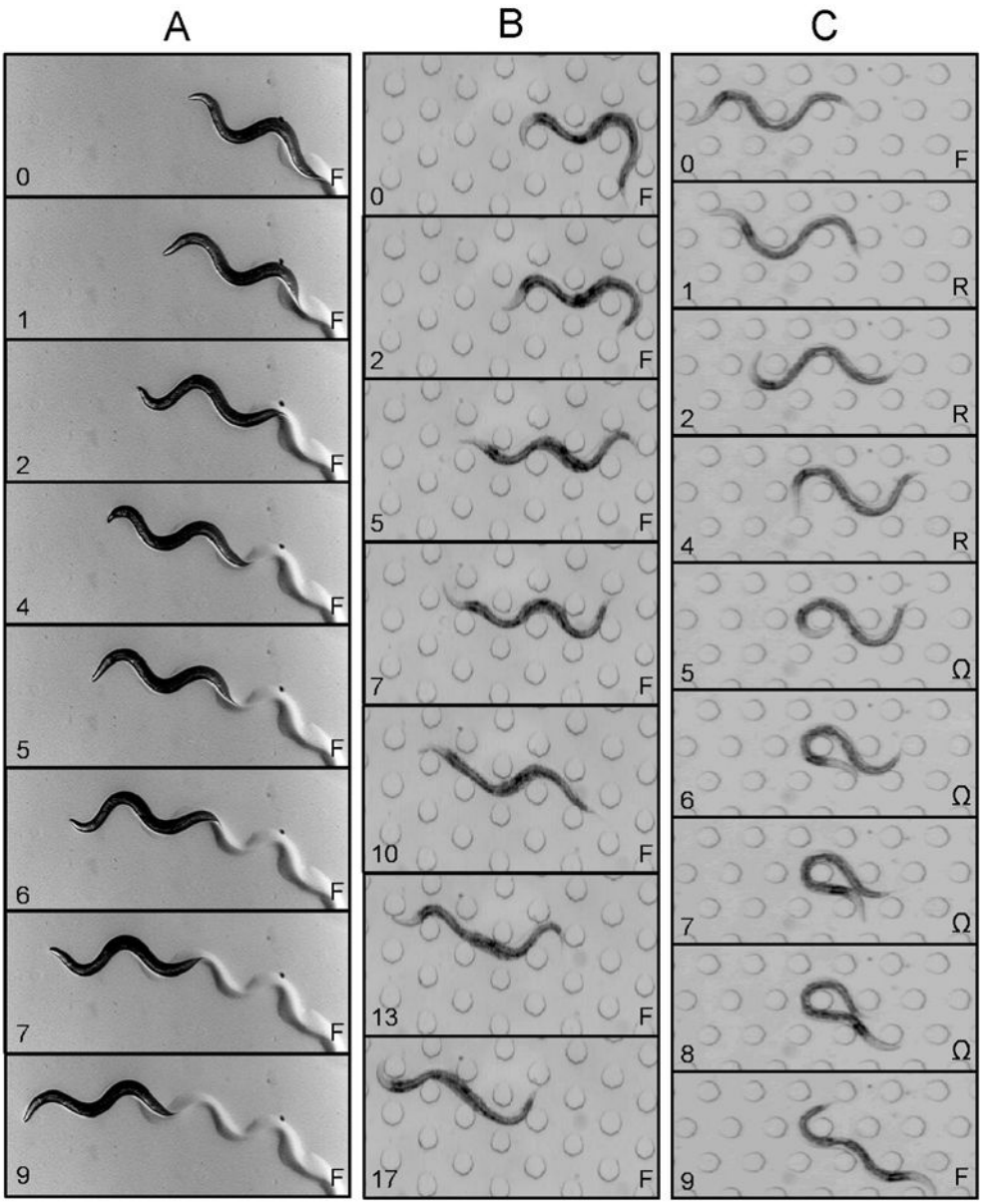

Figure 2.

Comparison between crawling on agarose and crawling in artificial soil. A. Agarose. B & C Artificial soil device. Elapsed time (sec) is indicated on the lower left of each frame. Behavioral state (F, forward crawling; R, reverse crawling; Ω, omega-turn) is indicated on the lower right. Post diameter is 100 μm; the minimum gap between posts is 100 μm. Panels B and C were taken from Supplemental Movies 1 and 2, respectively.

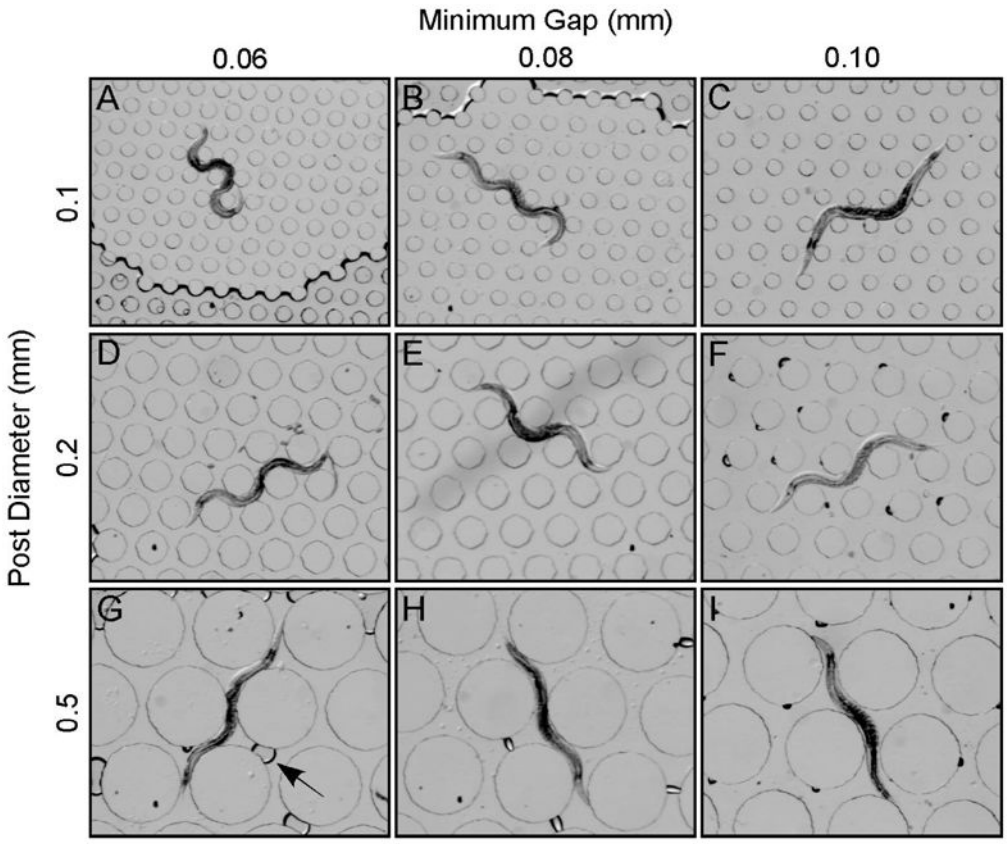

Figure 3.
Crawling behavior in nine artificial soil devices. A-G. Each device has a unique topography, defined by post diameter and the minimum gap between posts. Rows show devices with the same post diameter; columns show devices with the same gap. Post diameters and gaps are indicated in the margins. The slightly darker region at the bottom of A is an air pocket; the arrow in G points to an air bubble.

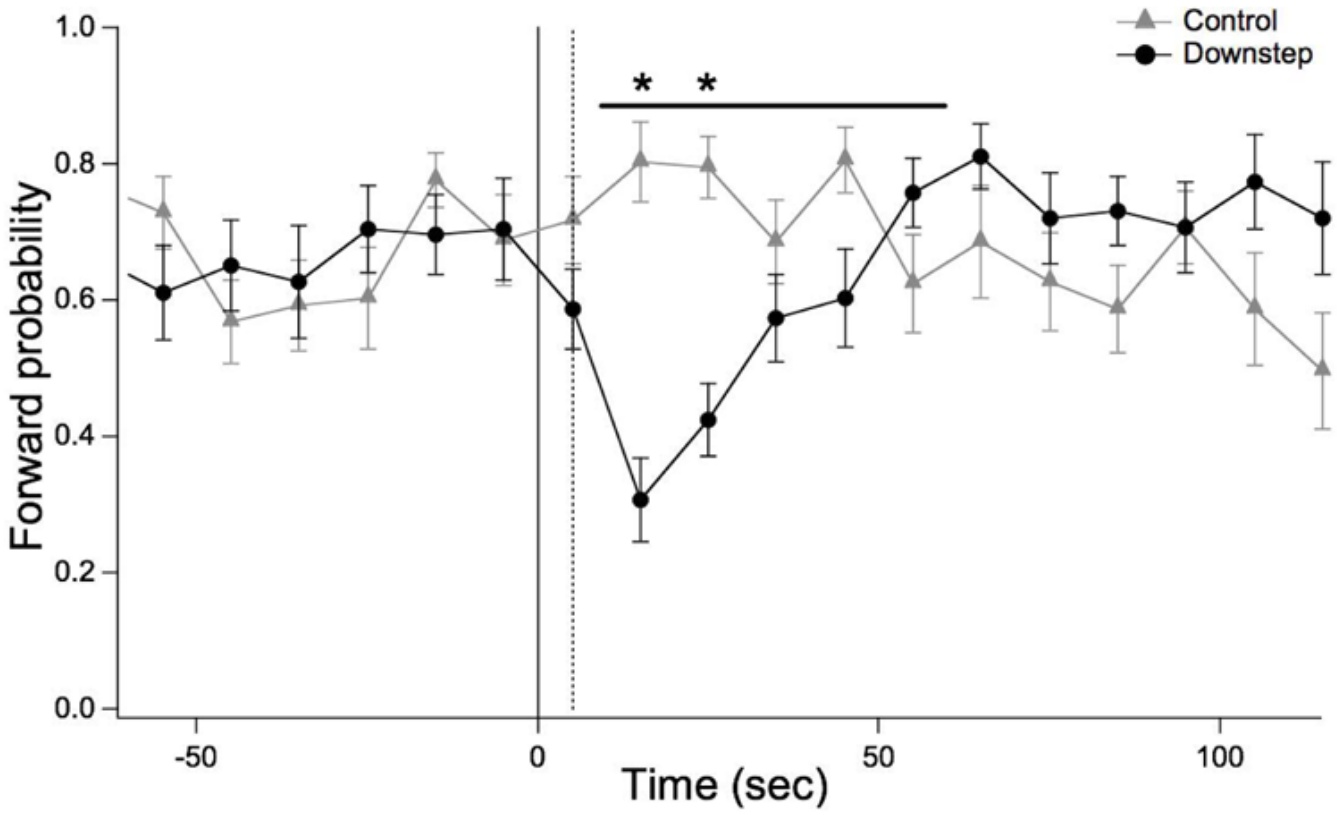

Figure 4.

Sodium chloride step-response behavior in the artificial soil device. The probability of forward crawling is plotted versus time in 10 sec bins. Perfusion was switched from Reservoir A to Reservoir B (see Fig. 1) at $t = 0$. The dashed line shows the time at which the front of Solution B reached the center of the device, as determined in separate experiments using food dye. In the Downstep group (20 worms), NaCl concentrations in Reservoir A and B were 100 mM and 1 mM respectively. In the Control group (20 worms), both solutions were 100 mM NaCl. *Statistics*. ANOVA in the window indicated by the horizontal bar: main effect of treatment, $F(1,38)$, $p < 10^{-5}$. Asterisks: *Post-hoc t*-tests after Bonferroni correction, $p < 0.05$.

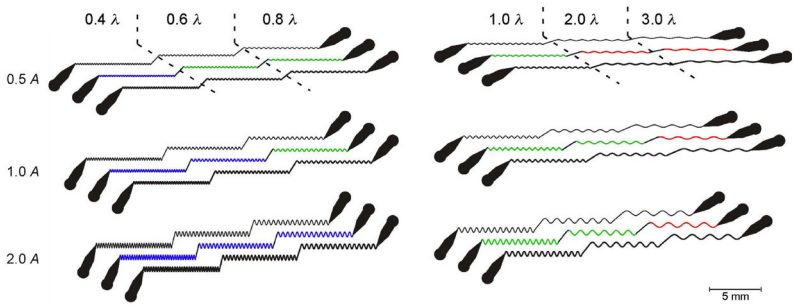

Figure 5.

Diagram of the waveform sampler device. The device consists of sinusoidal channels grouped into six triplets. Within a triplet, a single design is replicated with channels widths of 60, 80, and 100 μm (top to bottom). Each design comprises three sinusoidal domains connected by straight segments. Each domain has a unique combination of wavelength and amplitude (peak-to-peak), as indicated by the scale factors in the margins. The scale factors are nominally wild-type values of amplitude (A = 200 μm) and wavelength (λ = 500 μm). Domain color represents qualitatively distinct behaviors of worms in the channels: green, crawling with a well controlled waveform; blue, crawling with a partly controlled wave form; red, no crawling.

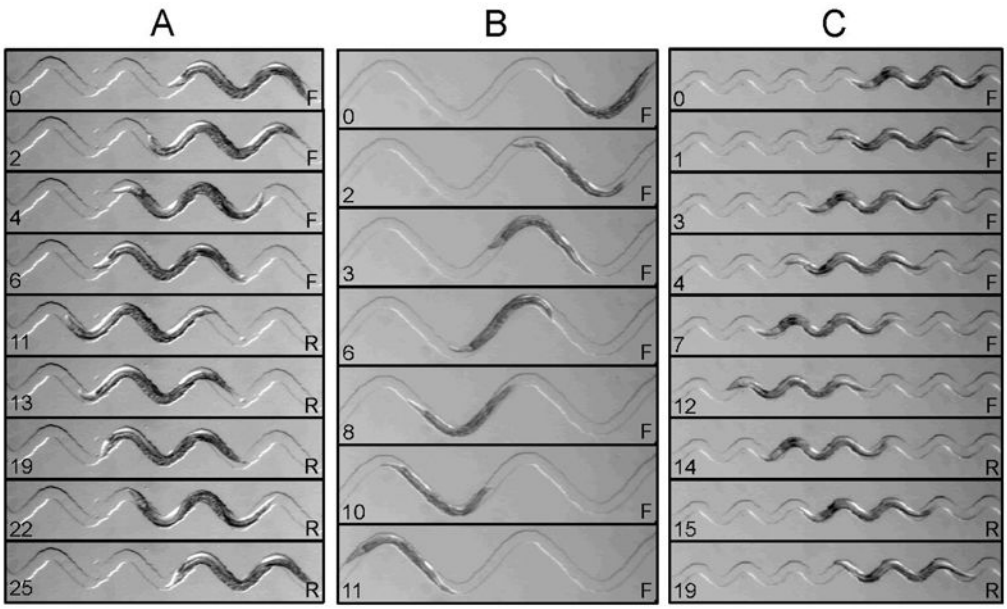

Figure 6.

Crawling behavior in waveform sampler device. Shown are three different channel domains in which waveform was well controlled by the channel. A. Wild-type waveform (1.0 *A*, 1.0 λ). B. Low thrust (low *F*, see text) waveform (2.0 *A*, 2.0 λ). C. High thrust (high *F*, see text) waveform (0.5 *A*, 0.6 λ). Elapsed time (sec) is indicated on the lower left of each frame. Behavioral state (F, forward crawling; R, reverse crawling) is indicated on the lower right. Channel widths (in μm): A, 80; B, 80; C, 60. A = 200 μm; λ = 500 μm. Panels A, B, and C were taken from Supplemental Movies 3, 4, and 5, respectively.

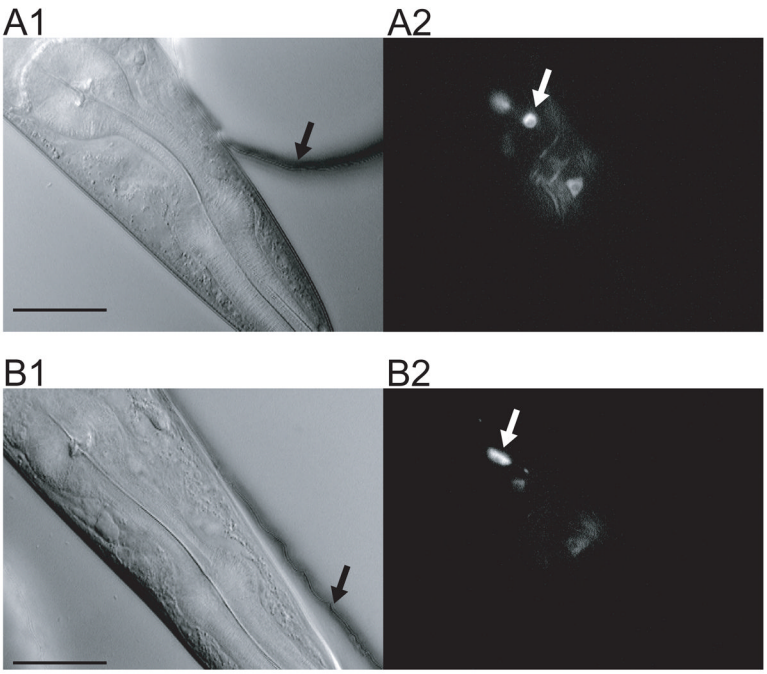

Figure 7.

Neuronal cell bodies imaged in the artificial soil and waveform sampler devices. A. Artificial soil. The worm was confined in the device shown in Fig. 3C. The *black arrow* indicates the wall of a post; the *white arrow* indicates a neuron cell body. B. Waveform sampler. The worm was confined in the channel shown in Fig. 6A. Arrows have the same meaning as in A. *Left*, differential interference contrast (DIC) image. *Right*, fluorescence image. Images were taken using Zeiss Axioskop FS equipped with a video camera (Dage MTI VE1000, Michigan City, IN). Fluorescence images are averages of five frames (29.98 frames/sec). Scale bar, 30 μm.